Journal of Hydroscience and Hydraulic Engineering
Vol. 9, No. 2, January, 1992, 59-72

FIELD MEASUREMENTS OF TURBULENT FLOW IN CHANNELS AND RIVERS

By

Tetsuro TSUJIMOTO

Associate Professor, Department of Civil Engineering, Kanazawa University
2-40-20, Kodatsuno, Kanazawa, 920, Japan

Tadanori KITAMURA, Toshiharu OKADA

Graduate Students, Department of Civil Engineering, Kanazawa University
2-40-20, Kodatsuno, Kanazawa, 920, Japan

and

Yoshinori OUJI

Nihon Suido Consultants Co. Ltd., Tokyo, Japan

ABSTRACT

Field measurements of turbulent flow are carried out in rivers and channels with electromagnetic anemometers. A set of two probes of the instruments can detect the three components of turbulent flow velocity simultaneously, and thus the turbulent characteristics of flows which are almost one order larger in length-scale than flows in laboratory flumes can be measured. The following flows are investigated: (i) uniform flows: (a) with sufficient submergence, (b) with small relative submergence, and (c) over vegetated beds; (ii) flow with abrupt change of bed roughness; and (iii) flow in a stream with vegetated zone in the cross-section. The obtained data are compared with those previously obtained in the laboratories, and discussed.

INTRODUCTION

The authors are involved in study on the turbulent structure of flows (i) with small relative submergence (6, 7), (ii) over vegetated bed (8, 12), and (iii) with abrupt change of bed roughness (13) based on turbulent measurements in small laboratory flumes. The data obtained in laboratory flumes were limited to those under condition of comparatively small Reynolds number ($Re \cong 10^4 \sim 10^5$, $Re \equiv Uh/\nu$; U=depth-averaged velocity, h=flow depth; and ν=kinematic viscosity). In the fields, at least the data with a few order higher Reynolds number would be obtained. Recently a small electromagnetic anemometer has been developed by which three components of turbulence can be measured without any special skills, though the reliability as for the turbulence characteristics has not necessarily been confirmed yet. The probe of this instrument (a cylinder, the length and the diameter of which are 3cm and 8mm, respectively) is still too big for a small laboratory flume (The flume in which the above researches were conducted was 0.4m wide, and thus the flow depth was limited at highest under 10cm), but it is sufficiently small if it is used in channels or rivers in the fields. The instrument is so durable to be used in the fields.

The study forcussed on the following flows: (a) uniform flow with sufficient submergence; (b) uniform flow over a gravel bed (with small relative submergence); (c) uniform flow over a vegetated bed; (d) flow with abrupt change of bed roughness; and (e) longitudinally uniform flow in a cross-section a part of which is covered by vegetation. The measuring sites were selected near the laboratory (Kanazawa University) considering the above flow conditions.

Turbulence measurements in the fields were attempted by several researchers since the age when the measuring technique was insufficient. Recent development of measuring devices such as electromagnetic anemometers and ultrasonic anemometers has made refined field measurements of turbulence comparatively easy and some data have been already published (Matsuoka (4), Kanda & Sera (3) and others). However, it seems difficult to distinguish the effect which causes the turbulent structure

from effects due to many other factors which are often inevitably included in the flows in real rivers. In this study, the measuring sites were carefully selected so that the flows were predominantly subjected to an obvious factor. In other words, the flows with one of predominant properties (b)~(e) were extracted and compared with the flow with (a).

MEASURING SITES AND EQUIPMENTS

Velocity measurements were conducted by small electromagnetic anemometers (KENEK VM201). The detectors are cylindrical, the diameter and the length of which are 8mm and 3cm, respectively. There are two types of probes according to the arrangement of the detectors; L and I types (see Photo 1). The former can measure the vertical and the longitudinal components of turbulence velocity; while the latter can measure the longitudinal and the lateral components. The time constant was 0.05s and the signal from the anemometer was recorded into floppy disks by a digital data recorder (DRF-1, TEAC) at 20Hz during almost 1~2min for each point. The electric power was supplied from the car battery through an AD-transducer (Daisy SL130-12). The upper edge of the probes were inserted to a vertical acrylic pipe (almost 2m long) along which the scales were carved to see the elevation of the sensors of the probes. The pipes with probes were supported by a stepladder as shown in Photo 2 in streams. The flow disturbance by the legs of the stepladder hardly affected the velocity measurements. Another method is to set the pipe to the strong transverse structures such as a bridge. But the transverse structure is hardly portable, and in general the supporting point of the pipes are too high to prevent the vibration of the pipes. The measuring sites and the flow conditions are summarized in Table 1.

Table 1 Conditions of field measurements of turbulent flows

Case	River or Channel	width (cm)	depth (cm)	U (cm/s)	bed roughness
ST3	Kaneura-Yosui	150	66	48.9	concrete bed
ST4	Kaneura-Yosui	150	66	50.0	concrete bed
SO3	Kaneura-Yosui	140	38	58.0	gravels d=3cm
OY6	Onosho-Yosui	267	22	81.2	gravels $d\cong$7cm
ST7	Saigawa River (Okuwa)	1190	80	35.2	cobbles $d\cong$20cm
ST1	Kaneura-Yosui	143	28	70.7	closely vegetated
SO3	Kaneura-Yosui	127	31	54.9	closely vegetated
HK1	Irrigation channel (Higashi-Kanazawa)	123	26	61.2	sparsely vegetated
HK2	Irrigation channel (Higashi-Kanazawa)	129	26	64.2	sparsely vegetated
RS1	Saigawa River (Kamigiku)	700	40	88	rough to smooth cobbles** to paved*
RS2	Saigawa River (Kamigiku)	900	60	130	rough to smooth cobbles** to paved*
SR1	Tatsumi-Yosui (Wakunami)	200	18	50	smooth to rough concrete to gravel
TV1	Saigawa River (Hoshima)	750	$\cong$40	88	gravel ($d\cong$15cm) 2m wide vegetated zone neighboring main channel
TV2	Saigawa River (Hoshima)	950	$\cong$65	130	gravel ($d\cong$15cm) 2m wide vegetated zone neighboring main channel

($) U=depth averaged velocity; d=diameter of bed materials;
(*) concrete with cobbles of diameter 10cm, but the roughness height is around 1cm; (**) d=15-20cm; (***) d=3cm

Photo 1 Probes of electromagnetic anemometers

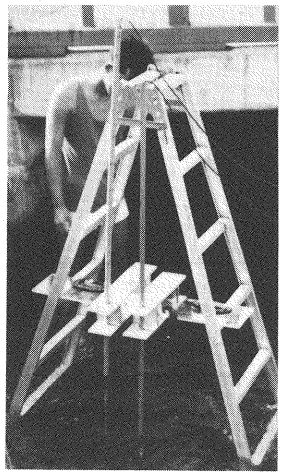

Photo 2 Turbulence measurements in the fields

TWO-DIMENSIONAL UNIFORM FLOW

Uniform Flow with Sufficient Submergence:

Cases ST3 and ST4 were measured at a concrete-made channel (Photo 3). The flows in the channel could be two-dimensional uniform flow.

Figure 1 shows the velocity and the Reynolds-stress distributions of flow. The Reynolds-stress distribution followed well a triangular one, and the shear velocity (u_*) was estimated from the extra-polated bed shear stress. The provisionally estimated values of u_* was used for making the velocity profile dimensionless and the inspection of the adaptability of the log-law supported that the provisionally estimated value of u_* was almost reasonable. The velocity, the Reynolds-stress and the turbulence-intensites distributions are made dimensionless by the estimated value of shear velocity in Fig.2. The velocity profile follows well the log-law.

$$\frac{u}{u_*} = \frac{1}{\kappa} \ln \frac{y}{h} + \frac{u_s}{u_*} \qquad (1)$$

in which u=local velocity; u_s=velocity at the free surface; and κ=Kármán constant (κ=0.4). In Fig.2, the extrapolated value was used for u_s. While, the turbulence-intensities distributions coincides to the exponential formulation proposed by Nezu (9) as follows:

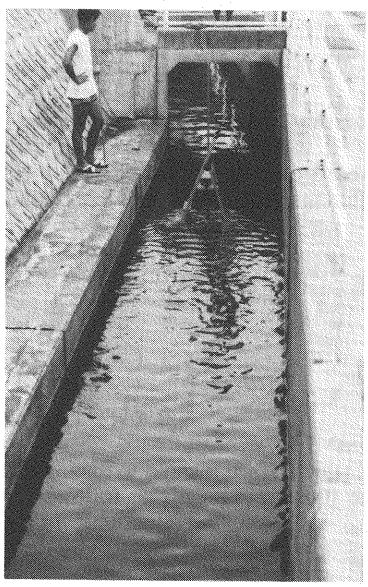

Photo 3 Concrete channel

$$\frac{u'_{rms}}{u_*} = 2.3\exp\left(-\frac{y}{h}\right); \qquad \frac{v_{rms}}{u_*} = 1.27\exp\left(-\frac{y}{h}\right); \qquad \frac{w'_{rms}}{u_*} = 1.63\exp\left(-\frac{y}{h}\right) \qquad (2)$$

in which u'_{rms}, v'_{rms}, w'_{rms}=turbulence intensities in the longitudinal, the vertical and the transverse directions; and h=flow depth. For Cases ST3 and ST4, the transverse component was not measured. The momentum exchange by turbulence is classified into 4 events (i) $u'>0$, $v'>0$; (ii) $u'<0$, $v'>0$; (iii) $u'<0$, $v'<0$; and (iv) $u'>0$, $v'<0$; in which u', v', w'=three components of turbulence. Among them, (ii) and (iv) bring the negative correlation of u' and v', and they contribute to the Reynolds stress. The

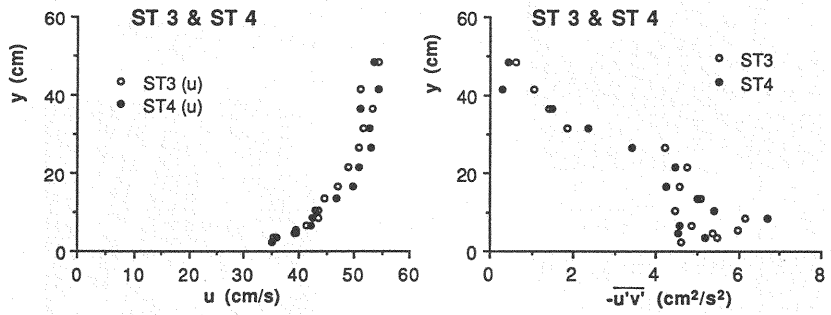

Fig.1 Velocity and Reynolds-stress distribution of flow with sufficient submergence

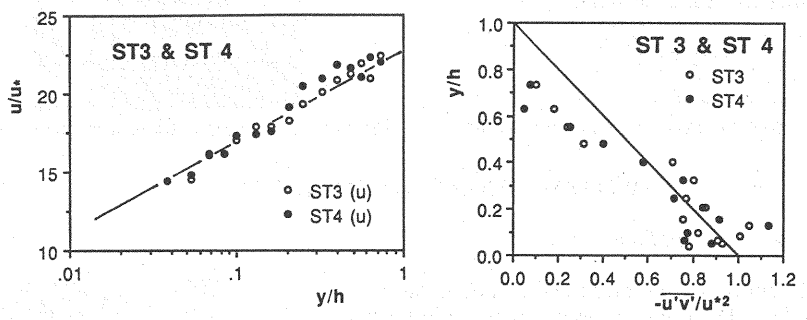

Fig.2(a) Dimensionless expressions of velocity and Reynolds-stress distribution

bursting, which brings the Reynolds stress near the boundary, is characterized by gradual "sweep" ($u'>0$, $v'<0$) and rapid "ejection" ($u'<0$, $v'>0$). In order to realize the bursting phenomenon from point measurements of turbulence, the following index is often inspected (Nakagawa & Nezu (5)):

$$RS_i = \frac{1}{\overline{u'v'}} \lim_{T\to\infty} \frac{1}{T} \int_0^T u'(t)v'(t)I_i(t,H)\mathrm{d}t \qquad (3)$$

$$I_i(t,H) = \begin{cases} 1 & (|u'v'| \geq H|\overline{u'v'}|) \\ 0 & (|u'v'| \leq H|\overline{u'v'}|) \end{cases} \qquad (4)$$

in which H= threshold to distinguish the bursting; and the subscript i means as follows: i=1: $u'>0$ and $v'>0$; i=2: $u'<0$ and $v'>0$ (ejection); i=3: $u'<0$ and $v'<0$; and i=4: $u'>0$ and $v'<0$ (sweep). By the turbulence measure-

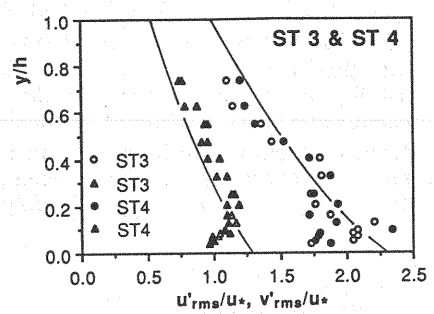

Fig.2(b) Dimensionless distribution of turbulence intensities

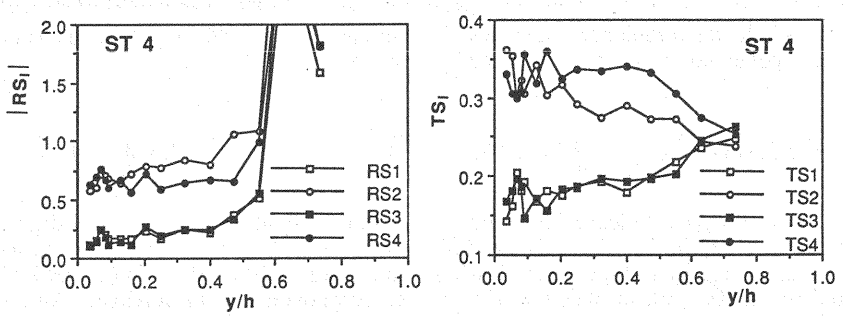

Fig.3 Contribution of each event of turbulence to Reynolds stress of flow with sufficient submergence

ment of flow over a smooth bed in the laboratory flume, Nakagawa & Nezu (5) demonstrated that "ejection" or event (ii) dominated near the bed.

Meanwhile, the time share of each event is obtained by the following equation.

$$TS_i = \lim_{T\to\infty} \frac{1}{T} \int_0^T I_i(t,H)\mathrm{d}t \qquad (5)$$

In Fig.3, the vertical distributions of the calculated $|RS_i|$ and TS_i are shown, where H=0 for simplicity, and the results are consistent with the flume data of Nakagawa & Nezu (5).

Uniform Flow over Gavel Bed with Small Relative Submergence:

In order to investigate the turbulent structure of flow with small relative submergence, the following sites were chosen: S02: alluvial bed with h=38cm, d=3cm, and thus h/d≅13; OY7: fixed bed composed of cobbles of d≅7cm with h=22cm (see Fig.4); and ST7: fluvial river covered by gravels of d≅10~20cm (see Photo 4) with h=80cm (h/d=4~8).

In Fig.5, distributions of the velocity and the Reynolds stress are shown. The Reynolds-stress distribution is no longer triangular near the bed. From an extrapolation of the data of the Reynolds-stress data away from the bed which followed a triangular one, the shear velocity (u_*) was estimated. Fig.6 shows the dimensionless distributions of the velocity, the Reynolds stress and the turbulence intensities. Fig.6 emphasizes that the velocity distribution becomes more uniform near the bed and that the Reynolds stress and the turbulence intensities are obviously suppressed from the expected one for flow with sufficient submergence also near the bed. In the field measurements, the theoretical bed (y=0) is difficult to determine, but it should exist near the top tangential level of gravel layer. The shift of the theoretical bed within the distance of the order of the gravel diameter hardly change the above characteristics pointed out from Fig.6. These facts were already pointed out by Nakagawa, Tsujimoto

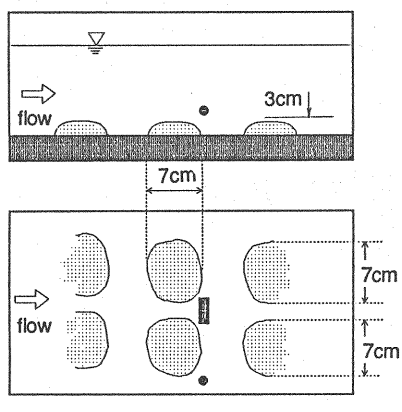

Fig.4 Bed roughness of Onosho-Yosui

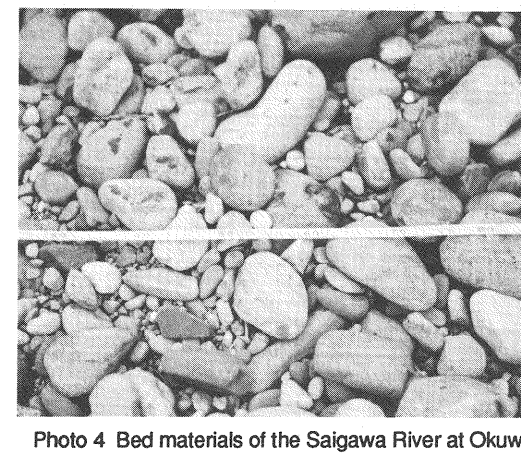

Photo 4 Bed materials of the Saigawa River at Okuwa

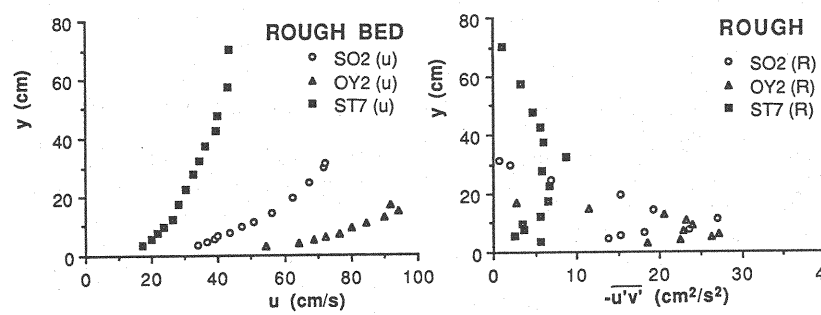

Fig.5 Velocity and Reynolds-stress distributions of flow over gravel bed

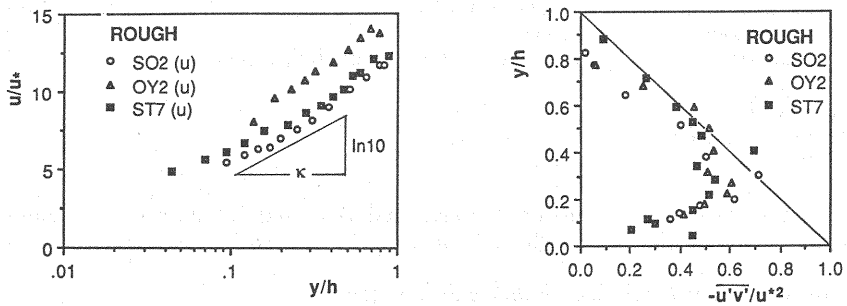

Fig.6(a) Dimensionless distributions of velocity and Reynolds stress

& Shimizu (6,7) as the characteristics of flow with small relative submergence from the flume experiments. They termed the region where the velocity was made uniform and the turbulence intensity and the Reynolds stress are suppressed "roughness sublayer." The present measurements clarified that the rough-ness sublayer exists in the flows with small relative submergence of the Reynolds number 1~2 order higher than the flows in the flumes.

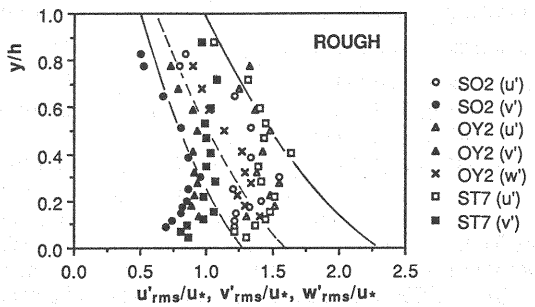

Fig.6(b) Turbulence -intensity distribution

Nakagawa, Tsujimoto & Shimizu (6) also investigated the contribution of each event of turbulence momentum exchange, and pointed pointed out that the event (iv) becomes more predominant than (ii) in the roughness sublayer and the so-called bursting phenomenon fades there. That implies that ejection fades away in the roughness sublayer. The results of the present measurements in the fields are shown in Fig.7, and the event (iv) obviously dominates over (ii) very near the bed.

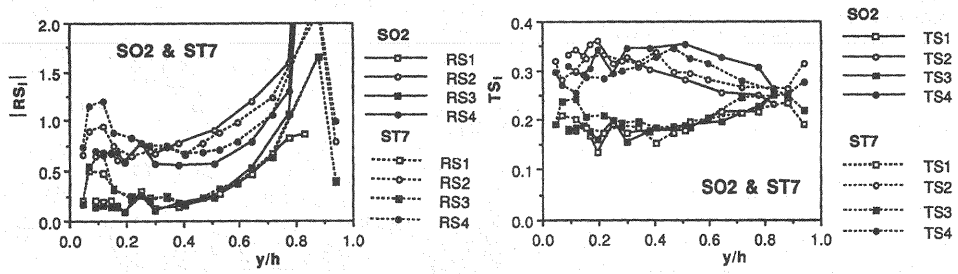

Fig.7 Contribution of each event of turbulence to Reynolds stress of flow over gravel bed

Uniform Flow over Vegetated Bed:

In order to investigate the turbulent structure of flow over a vegetated bed, irrigation channels were chosen for field measurements (Photo 5).

In Cases ST1 and SO3, the beds were covered closely by water plants (see Photos 6 and 7) as illustrated in Fig.8. In Cases HK1 and HK2, the beds were covered sparsely by water plants as illustrated by Fig.9. Both beds were composed of sand (d=0.3~0.6mm), but the water plants trail from the beds about 10% of the flow depth.

In Fig.10, the distributions of the velocity and the Reynolds stress are shown. By extrapolating the Reynolds-stress distribution to fit it to a triangular one for the region far from the bed, the bed shear

stress (at a sand bed) was estimated. The velocity, the Reynolds stress and the turbulence intensities were made dimensionless by the shear velocity obtained from the estimated bed shear stress, and plotted against the dimensionless height, y/h, in Fig.11. In logarithmic expression of the velocity distribution, y=0 was assumed to be the top-tangential plane for a closely vegetated bed (k in Fig.11 represents the vegetation-layer thickness); while y=0 was assumed to be the sand bed for a sparsely vegetated bed.

In the case of flow over a closely vegetated bed, both the Reynolds-stress and the turbulence-intensities distributions have peaks at the top-tangential plane of the vegetation layer, and those in the surface-flow region follows a triangular and exponential profiles respectively as similarly as the flow over a smooth bed. In the case of flow over a sparsely vegetated bed on the other hand, the Reynolds stress and the turbulence intensities are suppressed even in the surface-flow region just like the roughness sublayer. Though there cannot be recognized a uniformalization of the velocity in this region, it might depend on the definition of the theoretical wall.

In Fig.12, the contribution of each event to the turbulence momentum exchange is investigated for flow over a closely vegetated bed. Above the vegetation layer, the event (ii) is still active (the tendency of the roughness sublayer cannot be recognized), but in the vegetation layer (iv) is predominant instead of (ii).

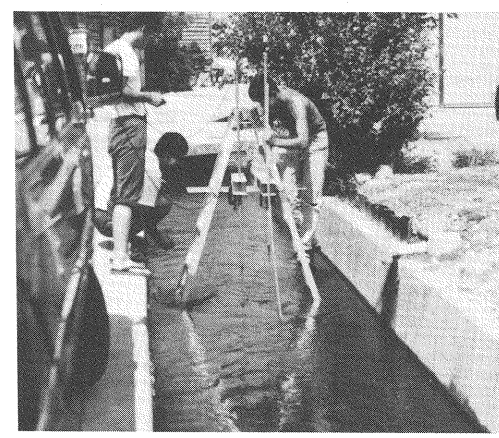

Photo 5 Vegetated bed channel

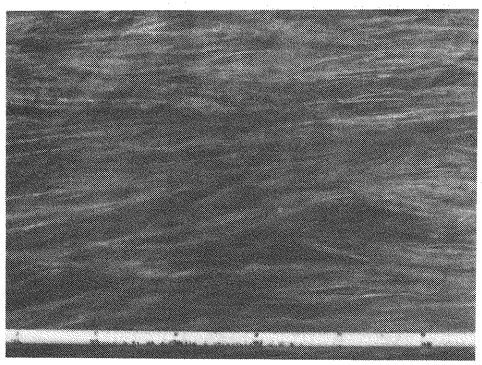

Photo 6 Water Plants lying on the bed

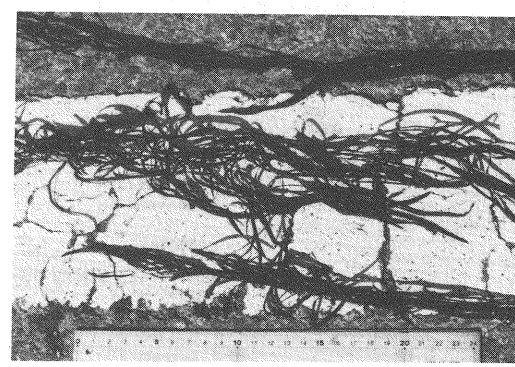

Photo 7 Water plants

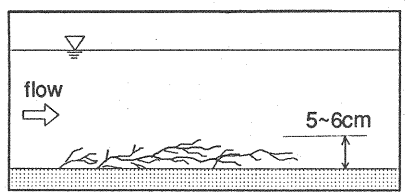

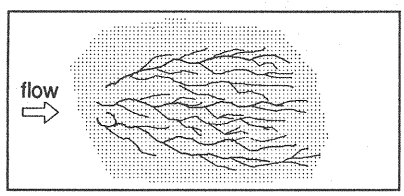

Fig.8 Illustration of closely vegetated bed

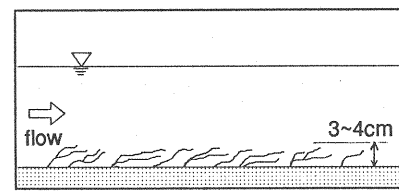

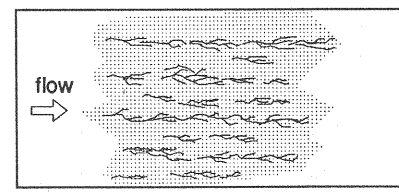

Fig.9 Illiustration of sparsely vegetated bed

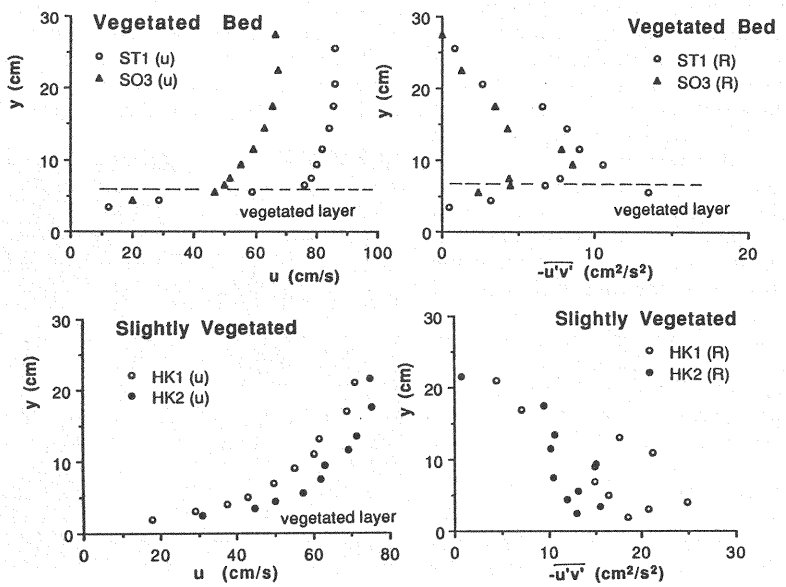

Fig.10 Velocity and reynolds-stress distributions of flow over vegetated bed

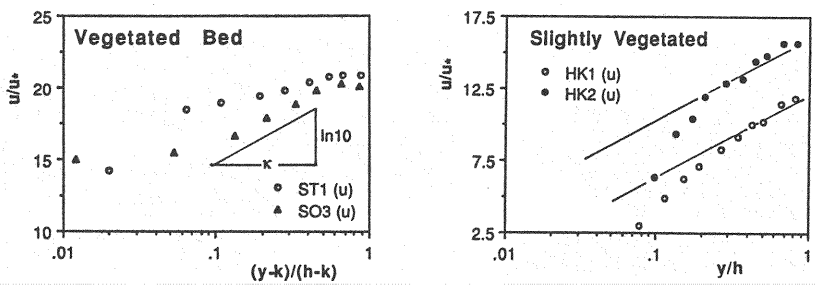

Fig.11(a) Dimensionless velocity distribution of flow over vegetated bed

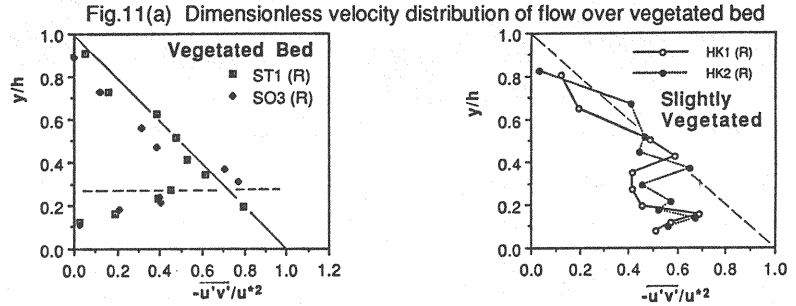

Fig.11(b) Dimensionless Reynolds-stress distribution of flow over vegetated bed

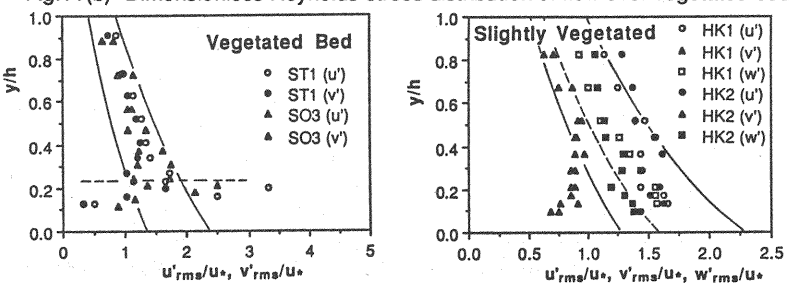

Fig.11(c) Dimensionless turbulence intensity distribution of flow over vegetated bed

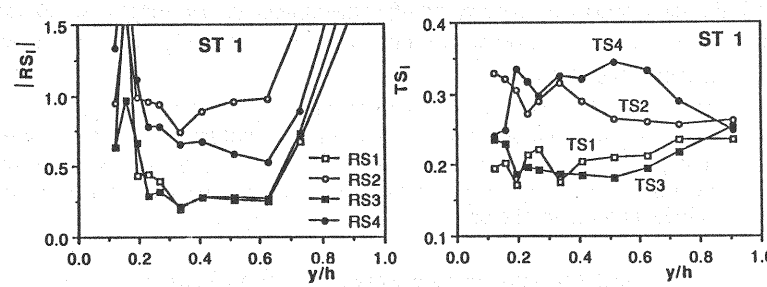

Fig.12 Contribution of each event of turbulence to Reynolds stress of flow over vegetated bed

These tendencies can be compared with the flume experiment. The outline of the data is consistent with the flume data (8, 12), but the detail has not been investigated.

TRANSITIONAL FLOW DUE TO ABRUPT CHANGE OF BED ROUGHNESS

In order to obtain field data of transitional flows due to abrupt change of bed roughness, the following sites were chosen: (a) the change of bed roughness from natural fluvial bed composed of gravels (d=15cm) to artificial rigid bed (roughness height was almost 2cm) in the Saigawa River near the Kamigiku Bridge (Case RS2 was measured at higher stage after a small flood than Case RS1); and (b) the change of bed roughness from concrete-made bed to alluvial flat bed composed of semi-fine gravel (d≅3cm) in the Tatsumi-Yosui near Wakunami-cho (SR1). Both sites had long uniform reaches upstream and downstream of the change of bed roughness. The turbulence measurements were conducted at various longitudinal distances from the point of change of bed roughness.

Figure 13 shows the longitudinal changes of the Reynolds-stress distribution. It is recognized that the extrapolated value of the Reynolds-stress to the bed (the bed shear stress) responds to the change of bed roughness almost immediately (an overshooting effect (8) is difficult to recognize quantitatively) and that it responds to the change with spatial lag which increases with the relative height.

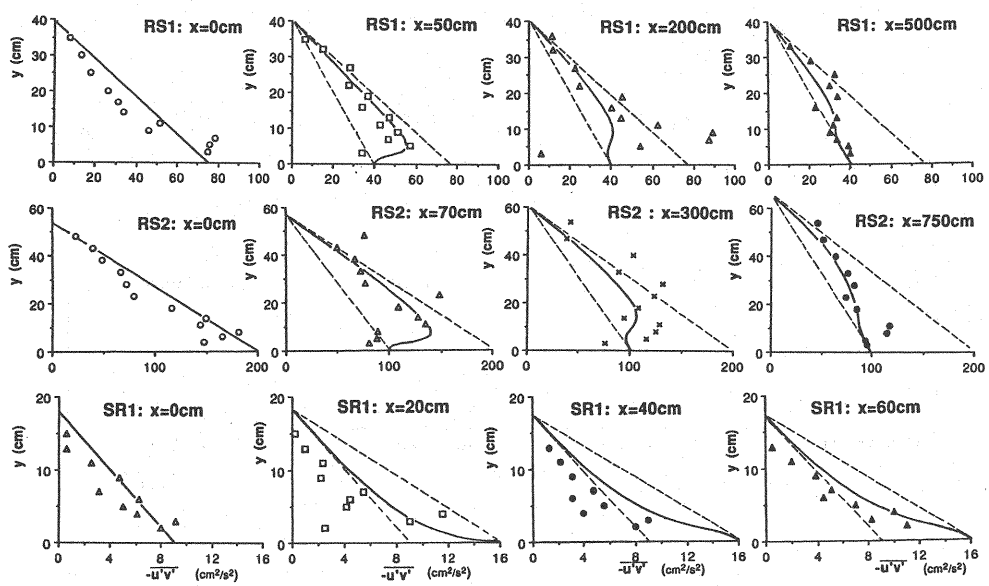

Fig.13 Transition of Reynolds-stess distribution due to abrupt change of bed roughness

From Fig.13, the shear velocities before and after the change of bed roughness, u_{*1} and u_{*2}, were estimated and indicated in Table 2 with other hydraulic parameters, in which u_s=surface velocity (extrapolated value from the data); and $\beta \equiv u_{*2}/u_{*1}$.

The change of the velocity profile in the transition process is shown in Fig.14, which are made dimensionless by using the estimated shear velocity after the change of bed roughness (u_{*2}). The velocity profile gradually changes from the log-law for the bed roughness upstream of the change gradually to the log-law for the bed roughness downstream of the change such that the velocity gradient adapts the new value increasingly from the bed.

Table 2 Change of shear velocity in field measurements

Case	bed condition	u_s (cm/s)*	h (cm)**	u_{*1} (cm/s)	u_{*2} (cm/s)	β
RS1	rough to smooth	110-120	34-42	8.7	6.3	0.72
RS2	rough to smooth	150-190	56-65	14.0	10.0	0.71
SR1	smooth to rough	52- 65	52-65	2.8	3.5	1.25

(*) range of surface velocity (surface velocity is extrapolated value); (**) range of flow depth

The authors (13) proposed a relaxation model for transient process of the Reynolds-stress distribution due to change of bed roughness, and its applicability to the flume data was confirmed.

According to the model, the change of the Reynolds-stress distribution can be expressed as follows (13):

$$\frac{\tau(\eta|\xi)}{\rho u_{*1}^2} = (1-\eta)[(\beta^2-1)\cdot\Psi(\eta|\xi)+1] \equiv (1-\eta)\cdot\Omega(\eta|\xi) \tag{7}$$

in which

$$\Psi(\eta|\xi) = 1 - \exp\left[-\frac{\xi}{\Lambda(\eta)}\right] \tag{8}$$

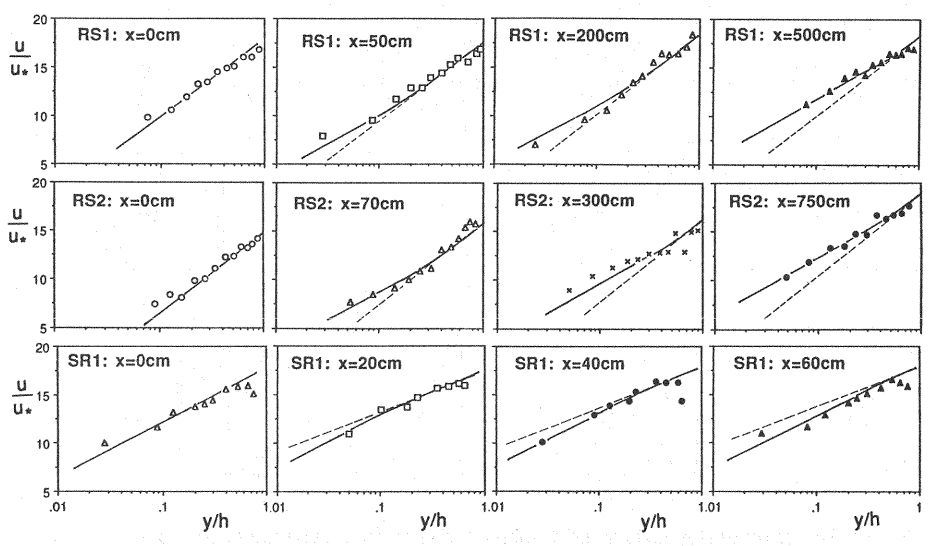

Fig.14 Transition of velocity profile due to abrupt change of bed roughness

$$\Lambda(\eta) = 20\eta(1+1.5\eta^3) \tag{9}$$

$\eta \equiv y/h$; $\xi \equiv x/h$; $\beta^2 \equiv \tau_{b2}/\tau_{b1}$; $u_{*1}=\sqrt{\tau_{b1}/\rho}$; and $u_{*2}=\sqrt{\tau_{b2}/\rho}$. $\Omega(\eta\,|\xi)$ is 1.0 for $\xi<0$, and $\Omega(\eta\,|\infty)\rightarrow\beta^2$. Thus, when $\xi<0$ or $\xi\rightarrow\infty$, the equilibrium appears.

The mixing length model is here applied even to the transitional flow with the following assumption of the mixing length which refers to the log-law for uniform open channel flow.

$$l^* = \kappa\eta\sqrt{1-\eta} \tag{10}$$

in which l^*=mixing length made dimensionless by flow depth. Then, the following velocity distribution is deduced for the transitional flow (13).

$$\frac{\partial}{\partial\eta}\left[\frac{u(\eta\,|\xi)}{u_{*1}}\right] = \frac{1}{\kappa\eta}\sqrt{\Omega(\eta\,|\xi)} \tag{11}$$

In Figs.13 and 14, the calculated curves based on the relaxation model are depicted and these well explain the change of the profiles.

FLOW WITH VEGETATION ZONE IN A CROSS-SECTION

In the Saigawa River, we found a sufficiently long uniform reach (≅70m, see Photo 8), of which the cross-section was a wide trapezoid with vegetated part (see Photo 9 and Fig.15). The authors (11) are studying the transverse mixing in the flow in a cross-section a part of which is vegetated, through a flume experiment. The present site is an ideal prototype of such a flume experiment.

For simplicity, the flow was regarded to be horizontally 2-dimensional. Instead of the depth-averaged velocity, the velocity at 60% depth was measured transversely. In Fig.16 the transverse distributions of the longi-longitudinal velocity U, the turbulence intensities (U'_{rms} and W'_{rms}) and the Reynolds stress ($-\overline{U'W'}$) are plotted. z is the transverse axis, and z>0 corresponds to the non-vegetated zone. Horizontal shear flow was recognized in the measured velocity profile which was well known through the flume experiments (2, 11, 15). The Reynolds-stress ($-\overline{U'W'}$, the transverse mixing of longitudinal momentum) has a peak at the interface between non-vegetated and vegetated zones, and it decreases with the transverse distance from the interface rapidly in the vegetated zone but gradually in the non-vegetated zone. The differences between the turbulence

Photo 8 The Saigawa River at Hoshima

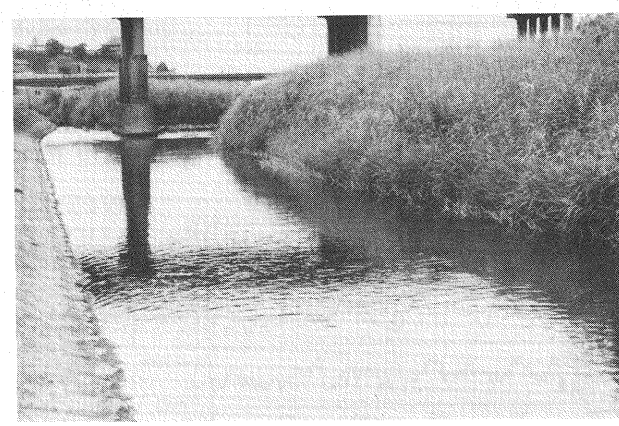

Photo 9 Measuring section in the Saigawa River

intensities in the vegetated zone and those in the non-vegetated zone are so large that no appreciable excess of the turbulence intensities near the interface was recognized.

In the case of flow in a channel, a part of whose width is covered by vegetation while the other is smooth, an obvious water-surface fluctuation was observed in the flume experiments (1, 14) and it was expected to contribute to the transverse momentum exchange. Thus, in the field measurements, the water surface-fluctuation was recorded simultaneously with the turbulence velocity. It was measured by capacity limnimeters (CHT 4-10, KENEK),. The instruments were suspended from the step-ladder with the electromagnetic anemometer with the I-type probe.

In Fig.17, examples of time series of simultaneous measurements of the water surface (y_w) and the longitudinal and the transverse velocities (U, W) near the interface between the vegetated and the non-vegetated zones are shown. Though comparatively low-frequency organized

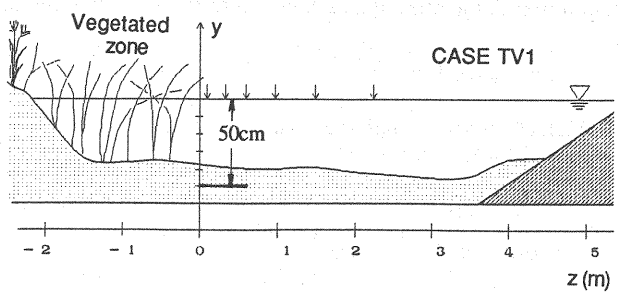

Fig.15 Illustration of cross-section of measuring site

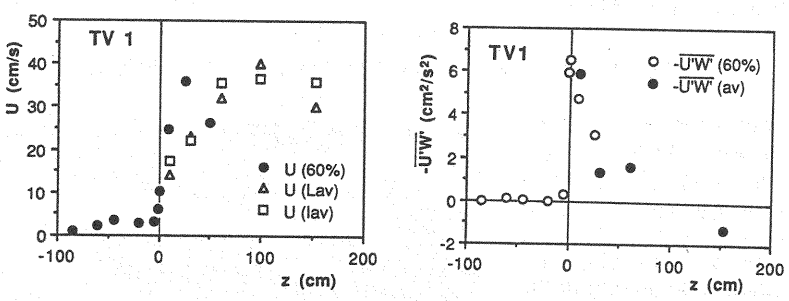

Fig.16(a) Transverse distribution of velocity and Reynolds stress

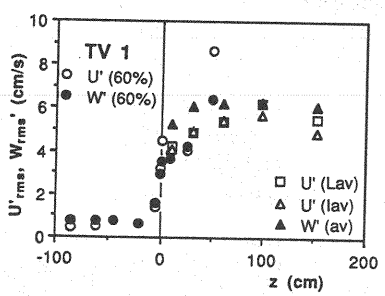

Fig.16(b) Transverse distribution of turbulence intensities

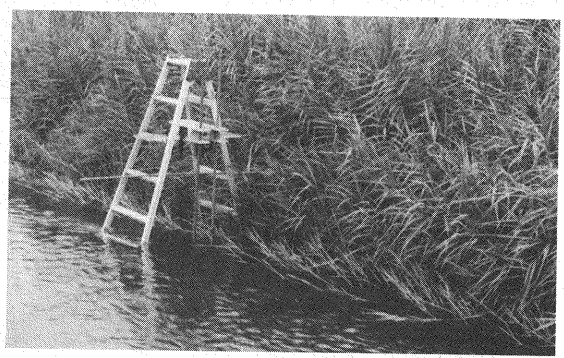

Photo 10 Turbulence measurements near vegetation zone

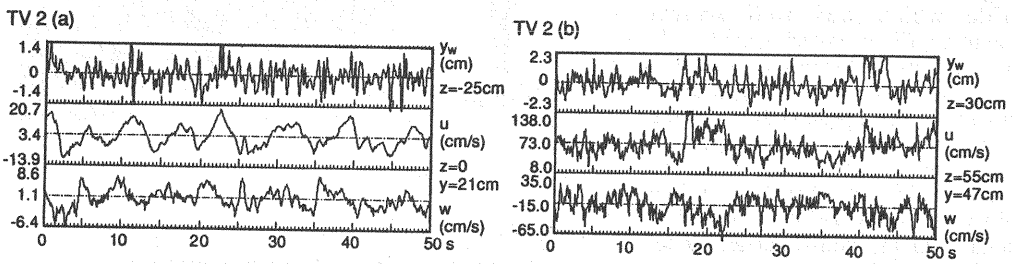

Fig.17 Time series of simultaneous measurements of water surface and longitudinal and transverse velocities near the interface between vegetated and non-vegetated zones

fluctuations would be recognized in the time series of y_w, U and W and they would be somewhat correlated, detailed investigations have not been accomplished yet.

CONCLUSIONS

The results obtained in this study are summarized below:

(1) For uniform flow with sufficient submergence, the data for the characteristics of turbulent flow over a smooth bed from electromagnetic anemometers were quite consistent with the data previously obtained through flume experiments.

(2) In the case of flow with small relative submergence, it was obtained through the flume experiments that the roughness sublayer appears, where the velocity profile is uniformalized and the turbulence intensities and the Reynolds stress are appreciably suppressed. The roughness sublayer and its characteristics were also recognized in the field measurements.

(3) In the case of flow over a closely vegetated bed, the Reynolds-stress and the turbulence intensities reach maxima at the upper boundary of the vegetation layer, and a triangular profile of the Reynolds-stress and exponential profiles of the turbulence intensities were recognized above it. On the other hand, in the case of flow over a sparsely vegetated bed, the Reynolds-stress profile was suppressed in a similar pattern to that in the roughness sublayer for flow with small relative submergence.

(4) In the fields, the turbulent characteristics of transitional flows due to abrupt changes of bed roughness were studied. The bed shear stress immediately responds to the bed roughness, and the Reynolds stress responds with a spatial lag which increases with the height from the bed. The relaxation model for the Reynolds-stress (9) could be applied to the field data without modifying the numerical parameters determined by flume data.

(5) Transverse distributions of the velocity, the Reynolds stress (the transverse turbulence flux of longitudinal momentum) and the turbulence intensities were measured in a uniform-flow reach in a river, a part of whose width was covered by vegetation in the fields. The flow was assumed horizontally two-dimensional. Organized water-surface fluctuations were also measured.

(6) Through the field measurements, it has been recognized that the recently developed electromagnetic anemometers are available to investigate the flow structure including the turbulence intensities and the Reynolds-stress distribution, though more detailed information about the turbulence structure cannot be investigated by them.

REFERENCES

1. Fujita, K. and S. Fukuoka : Lateral turbulent mixing in flood flow, *Proc. JSCE*, No.429/II-15, 27-36, 1991 (in Japanese).
2. Izumi, N., S. Ikeda and R. Ito : Effect of vegetation on flow and concentration of suspended sediment, *Proc. 33rd Jap. Conf. on Hydraul.*, JSCE, pp.313-318, 1989 (in Japanese).
3. Kanda, T. and M. Sera : Measurement of turbulence of river flows with ultrasonic flowmeter, *Proc. 3rd Int. Sym. Refined Flow Modeling & Turbulence Meas.*, Tokyo, Japan, pp.821-828, 1988.
4. Matsuoka, Y. : Turbulent structure of a gravel bed river, *Proc. 6th APD-IAHR Cong.*, Kyoto, Japan, Vol.II, pp.505-512, 1988.
5. Nakagawa, H. and I. Nezu : Prediction of contributions to the Reynolds stress from bursting events in open-channel flows, *Jour. Fluid Mech.*, Vol.80, No.1, pp.99-128, 1977.
6. Nakagawa, H., T. Tsujimoto and Y. Shimizu : Turbulent flow with small relative submergence, *Proc. Int. Workshop on Fluvial Hydraulics in Mountain Regions*, Trent, Italy, pp.A19-A30, 1989.
7. Nakagawa, H., T. Tsujimoto and Y. Shimizu : Experimental study on turbulent flow with small relative submergence, *Proc. JSCE*, No.423/II-14, pp.73-81, 1990 (in Japanese).
8. Nakagawa, H., T. Tsujimoto and Y. Shimizu : Open channel flow with water plants, *Proc. Hydraul. Engrg.*, JSCE, Vol.34, pp.475-480, 1990 (in Japanese).
9. Nezu, I. : *Turbulent Structure in Open-Channel Flows*, Doctoral Thesis, Kyoto Univ., 118p., 1977 (in Japanese).
10. Nezu, I., H. Nakagawa, K. Seya and Y. Suzuki : Response of velocity profile and bed shear stress to abruptly changed roughness in open-channel flows, *Proc. Hydraul. Engrg.*, JSCE, Vol.34, pp.505-510, 1990 (in Japanese).
11. Shimizu, Y., H. Nakagawa and Y. Iwata: Transverse velocity distribution of flow with vegetated zone, *Proc. 45th Annual Conf.*, JSCE, pp.313-318, 1989 (in Japanese).

12. Shimizu, Y., T. Tsujimoto, H. Nakagawa and T. Kitamura : Experimental study on flow over vegetated bed, *Proc. JSCE.*, No.435/II-17, pp.31-40, 1991 (in Japanese).
13. Tsujimoto, T., A.H. Cardoso and A. Saito : Open channel flow with spatially varied bed shear stress, *Jour. Hydroscience & Hydraul. Engrg.*, JSCE, Vol.8, No.2, pp1-20, 1990.
14. Tsujimoto, T. : Mixing process in open channel with vegetated region, *Proc. Int. Sym. on Environ. Hydraul.*, Hong Kong, 1991.
15. Yamazaki, S., T. Ishikawa and T. Kanamaru : Experimental study on horizontal shear flow in an open channel, *Proc. 39th Annual Conf.*, JSCE, II-237, pp.473-474, 1984 (in Japanese).

APPENDIX - NOTATION

The following symbols are used in this paper:

d	= diameter of bed materials;
h	= flow depth;
H	= threshold value to detect bursting;
k	= vegetation-layer thickness;
l^*	= mixing length made dimensionless by h;
Re	= Reynolds number;
RS_i	= contribution ratio to the Reynolds-stress of the i-th event;
TS_i	= time share of the i-th event in turbulent motion;
u	= local velocity in longitudinal direction;
u', v', w'	= turbulence velocity components;
u'_{rms}, v'_{rms}, w'_{rms}	= turbulence intensities in longitudinal, vertical and transverse directions;
u_s	= surface velocity;
u_*	= shear velocity;
u_{*1}, u_{*2}	= shear velocities before and after change of bed roughness;
U, W	= depth-averaged velocity components in longitudinal and transverse direction;
U'_{rms}, W'_{rms}	= depth-averaged turbulence intensities in longitudinal and transverse direction;
x, y, z	= longitudinal, vertical and transverse coordinates;
β	$\equiv u_{*2}/u_{*1}$;
κ	= Kármán constant;
Λ	= relaxation distance of Reynolds stress due to change of bed roughness;
ν	= kinematic viscosity of water;
ξ, η	$\equiv x/h$ and y/h, respectively;
ρ	= mass density of water;
τ, τ_b	= Reynolds stress and bed shear stress; *and*
Ω, Ψ	= defined by Eq.7 and Eq.8, respectively.

(Received July 18, 1991; revised December 16, 1991)